RSC Advances

This work reported the crystal structure, thermal decomposition, mechanical sensitivity and catalytic property of sodium complex of 5,7-diamino-4,6-dinitrobenzofuroxan.

Crystal Structure, Thermal Decomposition, Mechanical Sensitivity of Na[CL-14·2H₂O] and Its Catalytic Effect On the Thermal Decomposition of Ammonium Nitrate

Jian Cheng[1*], Yan Dong[2], Hui Ma[2], Lixia Li[3], Zuliang Liu[1*], Fengqi Zhao[4], Siyu Xu[4]

[1] School of Chemical Engineering, Nanjing University of Science and Technology, Nanjing, jiangsu 210094, P. R. China;

[2] Shijiazhuang No.4 Pharmaceutical Co.,Ltd., Shijiazhuang, 050021, China;

[3] School of Environment and Safety Engineering, Jiangsu University, Zhenjiang, Jiangsu 212013, P. R. China;

[4] Xi'an Modern Chemistry Research Institute, Xi'an, shanxi 710065, P. R. China

Corresponding author. Tel.: +86 25 8431 8865; fax: +86 25 8431 5030.

E-mail address: chengjian09@foxmail.com(J. CHENG).

ABSTRACT: A one-dimensional energetic complex (Na[CL-14·2H₂O]) constructed from sodium and 5,7-diamino-4,6-dinitrobenzofuroxan (CL-14) was synthesized, and its crystal structure was analyzed by X-ray diffraction. The crystal belongs to a monoclinic system with space group $P2_1/c$. The complex possesses a one-dimensional coordination framework based on $[ONaN]_n$ chain, which might result in its low sensitivity and high heat resistant. The thermal decomposition mechanism of Na[CL-14·2H₂O] was predicted by means of TG-DSC, TG-MS and FTIR analyses. The thermal decomposition of Na[CL-14·2H₂O] contains one endothermic and one exothermic processes in the temperature range of 25-500 °C with NaNCO, Na_2CO_3, H_2O, NO and CO_2 as the final products. The non-isothermal kinetic and thermodynamic parameters for the first exothermic process of the Na[CL-14·2H₂O] have been studied, with the apparent activation energy, pre-exponential factor, entropy of activation, enthalpy of activation and free energy of activation of 280.7 kJ/mol, 57.8, 282.7 J/mol K, 276.2 kJ/mol and 154.8 kJ/mol, respectively. The impact sensitivity and friction sensitivity of Na[CL-14·2H₂O] was tested according to general methods, with the values of 27 J and 360 N, respectively.

The Na[CL-14·2H$_2$O] has been incorporated as an energetic catalyst in ammonium nitrate (AN) by means of TG-DTG, TG-MS, DSC and extend of conversion (α)-T kinetic curves analyses. And the thermal kinetic constants for the catalytic and noncatalytic decomposition of AN samples were calculated by using Kissinger's and Ozawa-Doyle's equations. The possible catalytic mechanism was also discussed and proposed. The results show that Na[CL-14·2H$_2$O] decreases the peak temperature and activation energy value of completely decomposition process for AN by 41.3 ºC and 10.9 kJ/mol, respectively. Furthermore, the thermal decomposition of AN in presence of Na[CL-14·2H$_2$O] starts at significant lower temperature (about 30 ºC) than that of pure AN. Apparently, Na[CL-14·2H$_2$O] could be incorporated as a potential energetic catalyst in AN-based propellants.

Keywords: Energetic complex, 5,7-diamino-4,6-dinitrobenzofuroxan, crystal structure, thermal decomposition mechanism, energetic catalyst, ammonium nitrate

1. Introduction

The application of high energy, low signature and environmentally-friendly oxidants is the dominated developing trends of solid propellants for tactical missile motor. Ammonium dinitramide (ADN), NH$_4$[N(NO$_2$)$_2$] is currently the most promising of all green propellants because it is high energy and pollution-free compared with a common hydrazine propellants. ADN monopropellant, regarded as a new type of next-generation solid propellants, is more suitable for use in low-thrust engines [1]. Ammonium nitrate (AN) is widely used as fertilizer, industrial explosive ingredients and oxidants in solid propellants because it is relatively cheap, releases almost 100% gaseous products when it decomposes, and has a positive oxygen balance. Since the combustion products of AN does not contain noxious halides harmful to the environment, it is also considered as an environmentally-friendly and low signature oxidants. AN now is receiving a reinvigorated interest as a possible partial substitute for ammonium perchlorate (AP) in solid propellants [2-6]. However, compared to AND, low energy, low burning rate and the near room temperature polymorphic transitions limit the application of AN in solid propellants.

The near room temperature polymorphic transitions can be overcome by the use

of phase-stabilized AN, which can be prepared by methods like doping AN with various additives (such as metal oxides and metal salts) [7-23]. However, the drawback of these additives is obvious, most of them are non-energetic, an increase in their concentration might lead to decrease the total energy and burning rate of the AN based solid propellants. Work by Singh shows that transition metal salts of 5-nitro-2,4-dihydro-3H-1,2,4-triaole-3-one (NTO) were found to be promising for application in AN based solid propellants [24]. When these energetic salts are incorporated in AN based solid propellants, the corresponding metal oxides are produced *in situ* during thermal decomposition, which were found to have better catalytic activity on the combustion of AN based solid propellants. However, there are not many real cases and academic research papers in this area.

In the last few decades, a variety energetic metal complexes and salts of NTO, picric acid (PA), trinitroanilino benzoic acid (TABA), 2,4-dinitroimidazole, 2,6-diamino-3,5-dinitropyridine-1-oxide (ANPyO) and 2,6-diamino-3,5-dinitropyrazine-1-oxide (LLM-105) had been reported[24-35]. Some of these energetic metal complexes and salts exhibit excellent properties such as high energy, low sensitivity, high heat resistance and good catalytic effects on the combustion behavior of solid propellants, and could be incorporated as energetic catalyst in solid propellants. 5,7-Diamino-4,6-dinitrobenzofuroxan (CL-14) [36-37] is a high-performance energetic material that is thermally stable and insensitive to impact and friction, and whose explosive properties are superior to those of TATB. Mehilal [38] have reported the synthesis, characterization and energetic properties of four alkali metal salts (Na, K, Rb, and Cs) of CL-14 and compared their properties with those of alkali metal salts of 4,6-dinitrobenzofuroxan (DNBF). The preliminary data on alkali metal salts of CL-14 reveals that their thermal stability and sensitivity are superior to those of alkali metal salts of DNBF, while are inferior to that of CL-14. Furthermore, the crystal structures of these metal salts are not clear.

In accordance with previous studies on metal complexes of ANPyO and LLM-105, we deduce that CL-14 might form energetic complexes with a large number of metal ions due to its similar structure units (NH$_2$, N→O) and properties to

that of ANPyO and LLM-105. These new family of energetic complexes might exhibit excellent properties such as high energy, thermal stable and high decomposition heat, and might be incorporated as potential energetic catalyst in solid propellants. Thus, in this work, we reported a new sodium complex of CL-14 (Na[CL-14·2H$_2$O]), which has a completely difference coordination mode compared to that of ANPyO, LLM-105 and the other energetic materials-based metal complexes. The thermal decomposition mechanism, kinetic and thermodynamic parameters for the first exothermic process of Na[CL-14·2H$_2$O] were predicted base on TG-DSC, TG-MS and FTIR analyses. The Na[CL-14·2H$_2$O] has been incorporated as an energetic catalyst in AN-based propellants by means of TG-DTG, TG-MS, DSC, non-isothermal kinetic and extend of conversion (α)-T kinetic curves analyses. The possible thermal decomposition mechanism of AN catalyzed by Na[CL-14·2H$_2$O] was discussed and proposed.

2. Experimental

2.1. Materials and instruments

2-Nitroaniline (99.5%), sodium hypochlorite (98.0%), concentrated sulfuric acid (98.0%), concentrated nitric acid (98%-100%), hydroxylamine hydrochloride(99.9%), potassium bicarbonate (99.8%), sodium hydroxide (99.9%) and AN (AR) were obtained from Aladdin (shanghai, china). All reagents are of analytical grade and used without further purification.

The FTIR studies were conducted with use of a Bruker (55FT-IR) FTIR Spectrometer (500-4000 cm^{-1}). Elemental contents of carbon, hydrogen, and nitrogen were determined by a German Vario EL III analyzer. DSC analyses were recorded on a TA-DSC-Q20 from 25 to 500 ^{o}C, TG-DTG analyses were conducted on a TGA/SDTA851eMETTLER TOLEDO from 25 to 500 ^{o}C. TG-MS analyses were performed in a nitrogen atmosphere at a heating rate of 5 and 10 ^{o}C/min from 25 to 500 ^{o}C using a NETZSCH STA449C instrument.

2.2. Sensitive tests

The impact sensitivity and friction sensitivity measurements were made using a standard BAM Fall hammer and a BAM friction tester. [39].

2.3. Thermal decomposition and catalytic performance measurements of Na[CL-14·2H$_2$O]

The conditions of thermal decomposition (TG, TG-MS and DSC) measurements of Na[CL-14·2H$_2$O] (d_{50}: 4.5 um) were: sample mass, about 1.2-1.5 mg; N$_2$ flowing rate, 40 cm^{3}min^{-1}; heating rates (β), 2.5, 5, 10 and 20 ^{o}C/min; furnace pressures, 0.1 MPa; reference sample, α-A1$_2$O$_3$; type of crucible, aluminum pan with a pierced lid.

To test the catalytic effect of Na[CL-14·2H$_2$O] on the decomposition of AN, AN (d_{50}: 15.2 um) and Na[CL-14·2H$_2$O] (d_{50}: 4.5 um) were dry mixed (weight ratios 99:1) for 12 h. Then the resulting mixture was detected by TG-DTG, TG-MS and DSC measurements. The conditions of TG-DTG and DSC measurements of the mixture were: sample mass, about 1.0-1.2 mg; N$_2$ flowing rate, 40 cm^{3}min^{-1}; heating rates (β), 2.5, 5, 10, 15 and 20 ^{o}C/min, furnace pressures, 0.1 MPa; reference sample, α-A1$_2$O$_3$; type of crucible, aluminum pan with a pierced lid.

2.4. Synthesis

Synthesis of CL-14. CL-14 was prepared according to literature [36]. Anal. Calcd.(%):C, 28.02; H, 1.45; N, 32.72. Found: C, 28.07; H, 1.41; N, 32.80. IR, (KBr, cm^{-1}): 3350, 3245, 1620, 1606, 1552, 1512, 1344, 1295, 1247, 1211.

Synthesis of Na[CL-14·2H$_2$O]. CL-14 (0.295 g, 1.0 mmol) was added to a solution of NaOH (0.040 g, 1.0 mmol) in deionized water (30 mL) at 0-5 ^{o}C for 2.5 h, then filtered and washed with cool ethanol and air-dried. A yellow solid powder (0.298 g) resulted with a 95.0% yield (based on CL-14) and 0.12 g of this solid was dissolved in 15 mL methanol. Yellow crystal formed during slow evaporation of the solvent over a one week period. Anal. Calcd.(%):C, 22.93; H, 2.23; N, 26.75. Found: C, 22.90; H, 2.24; N, 26.76. IR, (KBr, cm^{-1}):3560, 3456, 3354, 3225, 1643, 1560, 1495, 1376, 1306, 1225, 1078, 1027, 971, 904, 824, 763, 677, 610, 475.

2.5. Crystallographic data collection and structure determination

The crystal structure was determined on a Siemens (Bruker) SMART CCD diffractometer using monochromatic Mo-Kα radiation (λ=0.71073 Å) at room temperature. All absorption corrections were performed by using the SADABS program [40]. Structures were solved by direct methods using the program

6

SHELXL-97 [41]. All non-hydrogen atoms were located in difference Fourier maps and refined anisotropically. All H atoms were refined isotropically, with the isotropic vibration parameters related to the non-H atom to which they were bonded. A summary of the structural determination and refinement for Na[CL-14·2H$_2$O] was listed in Table 1.

3. Results and discussion

3.1. Structural description of Na[CL-14·2H$_2$O]

Table 1 Crystal and experimental data of Na[CL-14·2H$_2$O]

Complex	Na[CL-14·2H$_2$O]
Empirical formula	C$_6$H$_7$NaN$_6$O$_8$
Formula weight	314.17
Crystal system	Monoclinic
Space group	$P2_1$/c
Temperature/K	293
a/Å	13.087(3)
b/Å	13.021(3)
c/Å	6.3070(13)
α/°	90.00
β/°	90.56(3)
γ/°	90.00
V/Å^3	1074.7(4)
Z	4
D_{calc}/g.cm^{-3}	1.942
$F(000)$	640
Limits of data collection /°	$1.56 \leq \theta \leq 25.39$
Reflections collected	1974
Independent reflections (R_{int})	1974(0.000)
Goodness of fit	0.978
R indices ($I > 2\sigma (I)$)	R_1=0.0725,wR_2 =0.1754
R indices (all data)	R_1=0.1209,wR_2 =0.2033

$$R_1= \Sigma| \ |F_o|\text{-}|F_c| \ |/\Sigma|F_o|. \ \omega R_2 = \Sigma[w(F_o^2\text{-}F_c^2)^2]/\Sigma[w(F_o^2)^2]^{1/2}$$
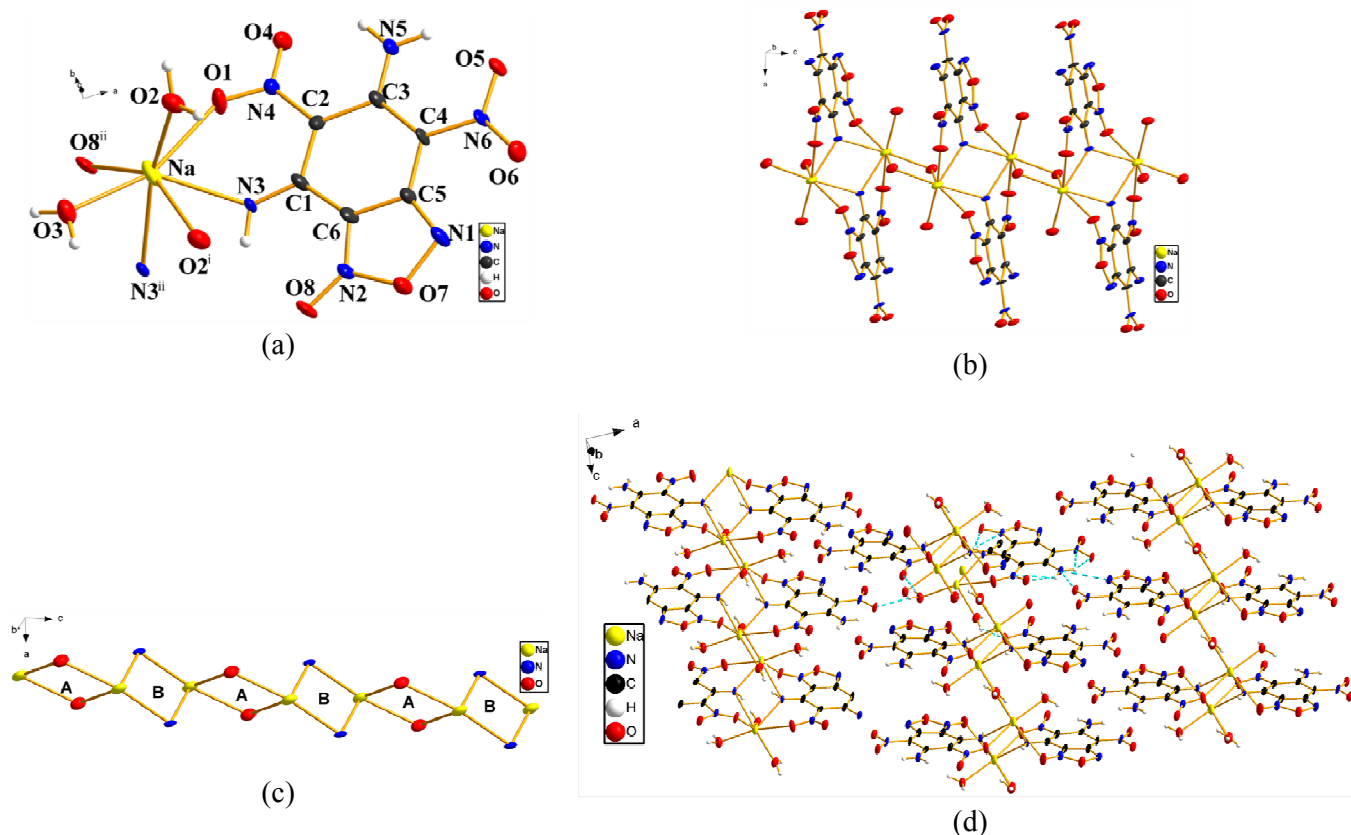

(a)

(b)

(c)

(d)

Fig. 1 A view of coordination environments in Na[CL-14·2H$_2$O] (symmetry code: i -x,-y,-z+1;ii -x,-y,-z) (a), View of 1D structure of Na[CL-14·2H$_2$O] (b), A view of the one-dimensional [ONaN]$_n$ chain along *c* crystal direction (c), A perspective view of the two-dimensional supramolecular structure of Na[CL-14·2H$_2$O] incorporating hydrogen bonds (dashed lines) (d).

Single crystal X-ray diffraction revealed that Na[CL-14·2H$_2$O] crystallizes in the monoclinic space group *P*2$_1$/c with an asymmetric unit consisting of a Na(I) cation, a single deprotonated H-C1-14 ligand and two coordinated water molecules. Selected bond distances and angles for Na[CL-14·2H$_2$O] are listed in Table 1 in supporting information. As shown in Fig. 1(a), Na(I) atom is coordinated by three oxygen atoms from three different water ligands (Na1–O2= 2.373(4), Na1–O3= 2.361(4), Na1–O2^i = 2.624(4) Å), two imine N atoms (Na1–N3=2.421(4), Na1–N3^{ii}= 2.539(4)) and two N→O O atoms (Na1–O1= 2.579(4), Na1–O8^{ii}= 2.842(4)) from two different C1-14$^-$ ligands to give a distorted NaN$_2$O$_5$ pentagonal bipyramid environment (symmetry code: (i) -x,-y,-z+1; (ii) -x,-y,-z).

In Na[CL-14·2H$_2$O], each CL-14$^-$ ligand links two Na^I cations through one imine N atom (N3) and two N→O O atoms (O1 and O8) with a μ_2-κ^3-O,N:N,O' binding mode. Two crystal lographically equivalent Na^I cations are bridged by two coordinated water molecules (O2) to form [(Na)$_2$(O)$_2$] rhomboid subunit–A, with a Na···Na separation of 3.908(5) Å. These rhomboid subunits are noticeably pinched, with Na–O–Na and O–Na–O angles of 102.7 (1) and 77.3 (1)^o, respectively. On the other hand, two symmetry-related Na^I cations are bridged by two imine N atoms (N3) to form a binuclear [(Na)$_2$(N)$_2$] rhomboid subunit–B. In subunit-B, the Na···Na separation is 4.028(5) Å, while Na–N–Na and N–Na–N angles are 108.6 (2) and 71.4 (2)^o, respectively. As shown in Fig. 1(c), adjacent Subunit-A and Subunit-B are interlinked to form a one-dimensional [ONaN]$_n$ chain extending along the *c* axis. Each [ONaN]$_n$ chain extends through C1-14$^-$ ligands, generating a one-dimensional coordination framework (Fig. 1(b)).

There are extensive inter- and intramolecular O–H···O, N–H···O and N–H···N hydrogen bonds connecting the one-dimensional chains of Na[CL-14·2H$_2$O] (Table 2 in supporting information). Six hydrogen bonds (N(3)-H(3B)···O(8), N(3)-H(3B)···N(2), N(5)-H(5A)···O(4), N(5)-H(5A)···N(4), N(5)-H(5B)···O(5) and N(5)-H(5B)···N(6)) exist in the chain. Neighboring one-dimensional chains are interconnected by O(3)-H(3D)···O(5)^{iii}, O(3)-H(3C)···O(4)^{iv}, N(5)-H(5A)···O(6)^v, N(5)-H(5B)···N(1)^v and O(2)-H(2A)···O(1)^{vi}, generating an extensive two dimensional hydrogen-bond network (Fig. 1(d)) [symmetry code: iii -1+x, y, z; iv -x, -1/2+y, 1/2-z; v 1-x, 1/2+y, 1/2-z; vi x, 1/2-y, 1/2+z.].

In general, Na[CL-14·2H$_2$O] has a completely difference coordination mode compared to that of ANPyO, LLM-105 and other energetic materials-based metal complexes [24-35]. CL-14 belongs to a multi-amino, multi-nitro-aromatic compound with symmetry molecular structure, which is close to that of well-known insensitive explosives such as TATB, LLM-105, ANPyO and 1,1-diamino-2,2-dinitroethene (FOX-7) [42]. The intramolecular, intermolecular hydrogen bonds are formed by the amino and nitro groups, resulting in a plane structure for CL-14. This may be the main reason for the good thermal stability and low sensitivity of CL-14. The π-electron

conjugated effect and the amino donor effect are also responsible for the good thermal stability and low sensitivity of CL-14. When the crystal structure of the Na[CL-14·2H$_2$O] went from the CL-14 plane layered structure to the one-dimensional coordination framework based on [ONaN]$_n$ chain. The intramolecular and intermolecular hydrogen bonds between amino and nitro groups might become weak, this is not conducive to reducing sensitivity and improving thermal stability of Na[CL-14·2H$_2$O]. While the link of C1-14$^-$ ligands through [ONaN]$_n$ chain which shows a similar pattern like the intermolecular hydrogen bonds formed by the amino and nitro groups of CL-14 might become strong, this helps reduce the sensitivity and improving thermal stability of Na[CL-14·2H$_2$O]. We conclude that the special coordination mode that the complex possesses a one-dimensional coordination framework based on [ONaN]$_n$ chain might result in its low sensitivity and high heat resistant compared to that of alkali metal salts of CL-14 [38].

3.2. Mechanical Sensitivity of Na[CL-14·2H$_2$O]

We tested the impact sensitivity and friction sensitivity of CL-14 and its sodium complex according to general methods, and compared this with that of trinitrotoluene (TNT). The results were shown in Table 2.

Table 2 Mechanical sensitivity test results of CL-14 and its sodium complex

compound	impact sensitivity/J	friction sensitivity/N
Na[CL-14·2H$_2$O]	27	360
CL-14	30	360
TNT[43]	15	353

As can be seen in Table 2, the impact sensitivity and friction sensitivity of CL-14 and its sodium complex is 30 J, 360 N, and 27 J, 360 N, respectively, which is significant lower than that of alkali metal salts of CL-14 [38]. According to the evaluation standard of the reference [39], the test results also indicate that both CL-14 and its sodium complex are less sensitive toward impact and friction than TNT, which reveals that both CL-14 and its sodium complex are classified as "less sensitive" energetic materials.

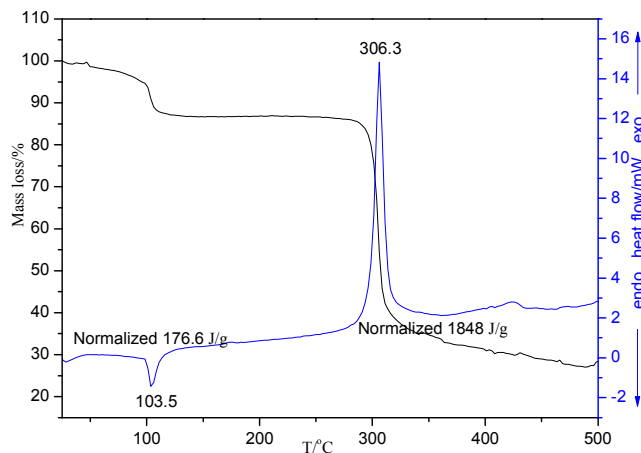### 3.3. Thermal decomposition mechanism of Na[CL-14·2H$_2$O]

Fig. 2 TG-DSC curves of the Na[CL-14·2H$_2$O] at the heating rate of 5 $^\circ$C/min
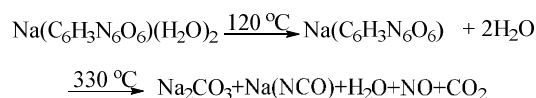
The TG-DSC curves of Na[CL-14·2H$_2$O] at the heating rate of 5 $^\circ$C/min were shown in Fig. 2. The FTIR spectrums of the solid residues for thermal decomposition of Na[CL-14·2H$_2$O] with nitrogen atmosphere at the heating rate of 5 $^\circ$C/min at different temperatures were shown in Fig. 1 in supporting information. The MS signals of gas products for thermal decomposition of Na[CL-14·2H$_2$O] with nitrogen atmosphere at the heating rate of 5 $^\circ$C/min were shown in Fig. 2 in supporting information. The FTIR spectrum of Na[CL-14·2H$_2$O] at room temperature, the stretching vibration absorption of $V_{(C-NO2)}$ peaks are at 1560 and 1376 cm^{-1} for the NO$_2$. The $V_{(NH2)}$ peaks are at 3456, 3225 and 1643 cm^{-1} for the NH$_2$. The $V_{(NH)}$ peak is at 3354 cm^{-1} for the NH. The $V_{(OH)}$ peak is at 3560 cm^{-1} for the H$_2$O. The $V_{(c=c)}$ peak is at 1587 cm^{-1} for the C=C. The $V_{(furoxan\ ring)}$ peaks are at 1495, 1225 and 1306 cm^{-1} for the furoxan ring. The $V_{(C-N)}$ peak is at 1241 cm^{-1} for the C-N. The $V_{(Na-N)}$ peak is at 475 cm^{-1} for the Na-N. The $V_{(Na-O)}$ peak is at 610 cm^{-1} for the Na-O.

The absorption peak of H$_2$O almost disappears at 120 $^\circ$C, while the other characteristic groups do not change. Corresponding to the TG-DSC curves, there is a mass loss of 12.8% in this process, which corresponds well with the calculation value of 11.5%. There is an endothermic stage in the range of 95.9-126.1 $^\circ$C with the peak temperature at 103.5 $^\circ$C from the DSC curve. Corresponding to the MS signals of gas products for the thermal decomposition of Na[CL-14·2H$_2$O], the peak at m/z=18 proves the presence of H$_2$O. This process would be the loss of two H$_2$O molecules

from the complex.

The exothermic stage occurs in the range of 268.6-338.5 ^{o}C with the peak temperature at 306.3 ^{o}C, which is significant higher than that of alkali metal salts of CL-14 [38]. This also indicates that Na[CL-14·2H$_2$O] is a heat resistant energetic material. Corresponding to this process, there is a mass loss of 52.0% from the TG curve. The cleavage of the amino-groups and nitro-groups can be confirmed by the disappearance of the absorption bands of $V_{(NH2)}$, $V_{(C-NO2)}$ and $V_{(NH)}$, respectively. The breaking of the benzene and furoxan rings can be confirmed by the disappearance of the absorption bands of $V_{(c=c)}$, $V_{(C=N)}$ and $V_{(N \to O)}$. The new absorption peaks at 2183, 1548,785 and 631 cm^{-1} prove the existence of NaNCO and Na$_2$CO$_3$ in the solid residues [29]. Corresponding to the MS signals of gas products for the thermal decomposition of Na[CL-14·2H$_2$O], the peaks at m/z=18, 30 and 44 prove the presence of H$_2$O, NO and CO$_2$ during this process. This process would be the Na-O, Na-N bonds breaking of the complex and the ring breaking of the ligands, which might be attributed to the completely decomposition of the Na[CL-14·2H$_2$O]. Furthermore, the overall heat of this process is 1848 J/g, which is significant higher than that of pure AN [24]. This indicates that an increase in its concentration might lead to enhance the total energy of the AN-based solid propellant.

On the TG curve, there still is a slow mass loss of 3.95% from 338.5 to 400 ^{o}C. Corresponding to this process, there are no obvious changes from DSC curve and FTIR spectrums. Therefore, the decomposition pathway of the Na[CL-14·2H$_2$O] might be described as follows:

$$Na(C_6H_3N_6O_6)(H_2O)_2 \xrightarrow{120\,^{o}C} Na(C_6H_3N_6O_6) + 2H_2O$$

$$\xrightarrow{330\,^{o}C} Na_2CO_3 + Na(NCO) + H_2O + NO + CO_2$$

3.4. Kinetic and thermodynamic parameters

Kinetic parameters. We studied the kinetic parameters of the first exothermic process of the Na[CL-14·2H$_2$O] by using Kissinger's [44] and Ozawa-Doyle's [45, 46] equations. The Kissinger and Ozawa-Doyle equations (1) are as follows:

$$\ln \frac{\beta}{T_p^2} = \ln(\frac{RA}{E}) - \frac{E}{R} \bullet \frac{1}{T_p}$$

$$\lg \beta + \frac{0.4567E}{RT_p} = C \qquad\qquad (1)$$

Where T_P is the peak temperature, K; R is the gas constant, 8.314 J/mol K; β is the linear heating rate, $^{\circ}$C/min; C is a constant. Based on the multiple non-isothermal DSC curves obtained at four different heating rates of 2.5, 5, 10, 20 $^{\circ}$C/min, the values of the apparent activation energy (E_k and E_o) (where subscript k: Kissinger's equation: subscript o: Ozawa-Doyle's equation), the preexponential factor (A_k) and linear correlation coefficient $(R_k$ and $r_o)$ of the exothermic decomposition process were determined by Kissinger's and Ozawa-Doyle's equations. The detailed data and the calculated kinetic parameters are listed in Table 3.

Table 3 Nonisothermal reaction kinetic parameters for the first exothermic process of Na[CL-14·2H$_2$O]

$\beta/(^{\circ}C/min)$	T_p/K	$E_k/(kJ/mol)$	$\ln(A_k)$	R_k^2	$E_o/(kJ/mol)$	r_o^2
2.5	570.24					
5	579.41					
10	582.75	280.7	57.8	0.9549	276.1	0.9578
20	590.79					

As can be seen in Table 3, the calculated results using both methods are within the normal range of the kinetic parameters of such thermal decomposition reaction, and correspond well with each other. Therefore, the Arrhenius equation of the exothermic decomposition process can be expressed in E_k and $\ln A_k$ as follows: $\ln k = 57.8 - 33.8 \times 10^3/T$.

Thermodynamic parameters. The entropy of activation ($\triangle S^{\neq}$), enthalpy of activation ($\triangle H^{\neq}$) and free energy of activation ($\triangle G^{\neq}$) corresponding $T=T_{po}$, $E=E_k$ and $A=A_k$ by equations (2), (3), (4) and (5) for the first exothermic process of Na[CL-14·2H$_2$O] were shown in Table 4, where K_B is the Boltzmann constant and h is Planck's constant [47-50]. We also compared this with that of 1,3,5,7-tetranitro-1,3,5,7-tetraazacyclooctane (HMX, d_{50}=90 um) [51].

$$T_{pi} = T_{po} + b\beta_i + c\beta_i^2 + d\beta_i^3 \quad i=1, 2, 3, 4 \qquad\qquad (2)$$

$$A\exp(\frac{-E}{RT})=K_B\frac{T}{h}\exp(\frac{-G^{\neq}}{RT}) \tag{3}$$

$$\triangle H^{\neq}=E- RT \tag{4}$$

$$\triangle G^{\neq}=\triangle H^{\neq} - T\triangle S^{\neq} \tag{5}$$

Table 4 Thermodynamic parameters of Na[CL-14·2H$_2$O] and HMX

compound	T_{Po}/K	E_k/(kJ/mol)	ln(A_k)	$\triangle S^{\neq}$ /(J/mol K)	$\triangle H^{\neq}$ /(kJ/mol)	$\triangle G^{\neq}$ /(kJ/mol)
Na[CL-14·2H$_2$O]	546.8	280.7	57.8	282.7	276.2	154.8
HMX	544.5	285.5	24.9	227.5	285.4	161.6

As can be seen in Table 4, some of the kinetic and thermodynamic parameters for Na[CL-14·2H$_2$O] (d_{50}: 4.5 um) are close to that of HMX (d_{50}=90 um) which is classified as a high heat resistant energetic material [51]. The kinetic and thermodynamic parameters of Na[CL-14·2H$_2$O] are within the normal range of the thermodynamic parameters for such thermal decomposition reaction. This indicates that Na[CL-14·2H$_2$O] is a high heat resistant energetic material, which is in agreement with the TG-DSC results of Na[CL-14·2H$_2$O].

3.5. Catalytic Effects of Na[CL-14·2H$_2$O] on the thermal decomposition of AN

To explore the potential application of the Na[CL-14·2H$_2$O] as an energetic catalyst in AN-based solid propellants, we studied the catalytic effects of Na[CL-14·2H$_2$O] on the thermal decomposition of AN. TG-DTG, DSC and kinetic parameters results for pure AN, AN in the presence of Na[CL-14·2H$_2$O] (AN/Na[CL-14·2H$_2$O]) were shown in Fig. 3, Fig. 4 and Table 5, respectively. TG-MS result of AN/Na[CL-14·2H$_2$O] was shown in Fig. 3 in supporting information.
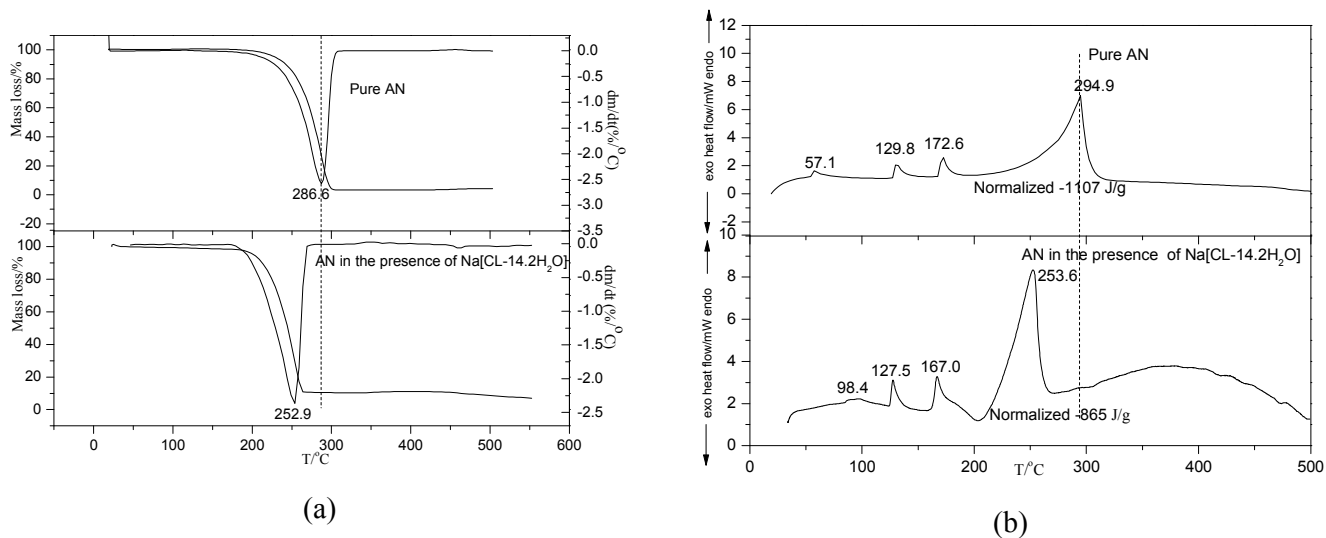
(a)   (b)

Fig. 3 TG-DTG (a) and DSC curves of AN and AN/Na[CL-14·2H$_2$O] at the heating rate of 10 ^{o}C/min (b)
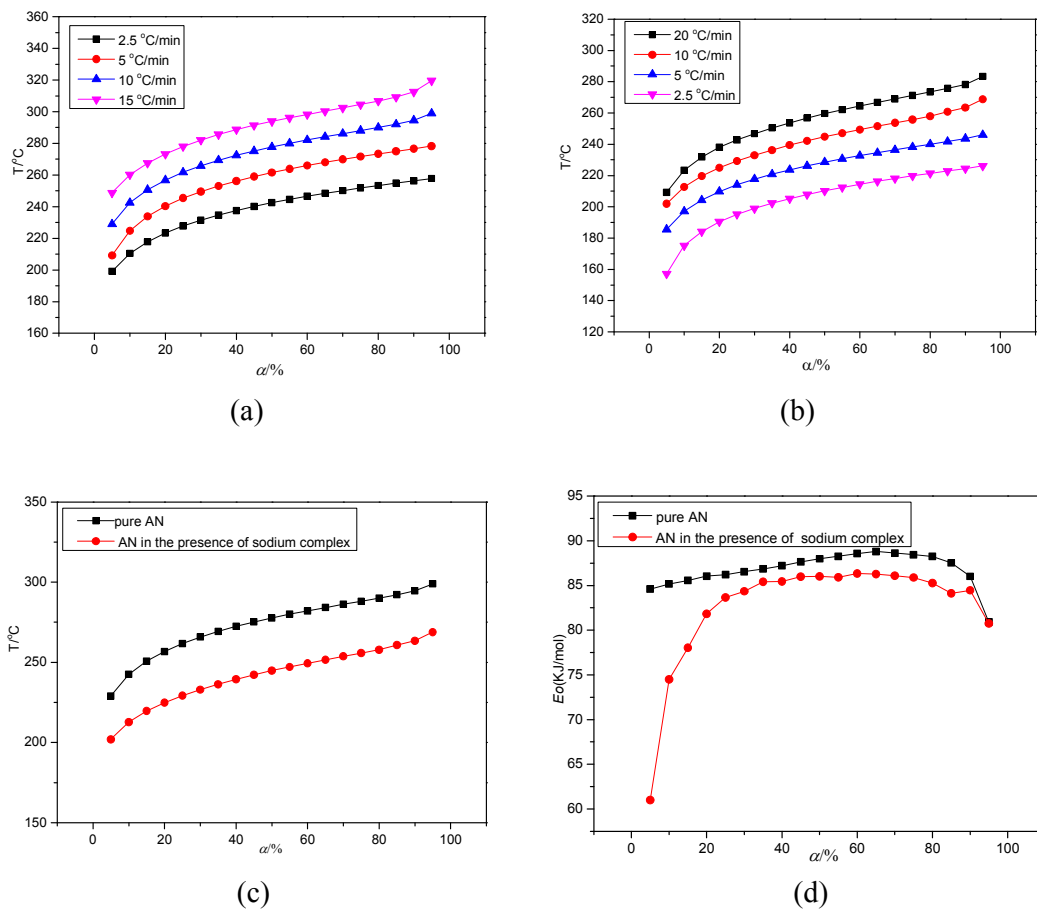

(a)   (b)

(c)   (d)

Fig. 4 α-T curves of pure AN at different heating rate (a), α-T curves of AN/Na[CL-14·2H$_2$O] at different heating rate (b), α-T curves of AN and

AN/Na[CL-14·2H$_2$O] at the heating rate of 10 ^{o}C/min, *Ea* of AN and AN/Na[CL-14·2H$_2$O] in different α (d)

Table 5 Summary of TG-DSC and Kinetic parameters results for pure AN, AN/Na[CL-14·2H$_2$O]

Sample	β/(^{o}C/min)	ΔH/(J/g)	T_0/^{o}C	T_p/^{o}C	T_e/^{o}C	E_a/(kJ/mol)	R_k^2
Pure AN	2.5	-1613	178.6	258.4	268.4	91.6	0.9874
	5	-1355	185.0	278.3	301.1		
	10	-1107	196.8	294.8	326.4		
	15	-1049	201.3	303.4	349.1		
AN/Na[CL-14·2H$_2$O]	2.5	-1343	172.3	224.4	235.7	81.0	0.9755
	5	-943	174.5	241.3	255.6		
	10	-865	201.6	253.5	267.9		
	20	-827	210.7	278.2	331.0		

Note: T_o, onset temperature of decomposition for DSC curve. T_e, end temperature of decomposition for DSC curve. T_p, peak temperature of decomposition for DSC curve.

TG-DTG, TG-MS and DSC analyses. As shown in Fig. 3, the DSC curve for pure AN reveals that the thermal decomposition of AN takes place in four steps: the endothermic phase transition at 57.1, 129.8 and 170.6 ^{o}C (contributed to phase transition of AN), the completely decomposition at 294.9 ^{o}C (contributed to intermediate products such as NH$_3$ and HNO$_3$ and a complete one to volatile products respectively) [15]. The overall heat for completely decomposition process is -1107 J/g, which is in agreement with the reported values [3]. Corresponding, the TG-DTG curves for pure AN reveal that the thermal decomposition of pure AN is a fast weight loss process, with about 97.0% mass loss from the initial mass in the temperature range of 193.9-311.6 ^{o}C, which reaches the largest rate at 286.6 ^{o}C. When Na[CL-14·2H$_2$O] is added, DSC curve of AN/Na[CL-14·2H$_2$O] reveals that Na[CL-14·2H$_2$O] additive has some effects on the phase transition temperature of AN: the endothermic phase transition at 57.1 ^{o}C shifts greatly to 98.4 ^{o}C, while the endothermic phase transition at 127.5 and 167.0 ^{o}C does not change greatly. This greatly shift of the phase transition temperature to higher side, from 57.1 ^{o}C to 98.4 ^{o}C, indicates that Na[CL-14·2H$_2$O] additive is effective for the phase stabilisation of AN. The endothermic stage occurs at about 100 ^{o}C might be contributed to the loss of two

H_2O molecules from the $Na[CL-14\cdot2H_2O]$. Corresponding to the MS signals of gas products for the thermal decomposition of $AN/Na[CL-14\cdot2H_2O]$, the peaks at m/z=17, 18, 30 and 63 prove the presence of NH_3, HNO_3, H_2O and NO during this process. Furthermore, as can be seen in Fig. 3, the peak temperature (253.6 ^{o}C) for $AN/Na[CL-14\cdot2H_2O]$ is 41.3 ^{o}C, which is lower than that of pure AN. Corresponding, the TG-DTG curves for $AN/Na[CL-14\cdot2H_2O]$ reveal that AN was completely decomposed at the lower temperature (201.6-253.5 ^{o}C) in a shorter time. The overall heat for completely decomposition (-865 J/g) is 242 J/g, which is higher than that of pure AN. Obviously, AN decomposition is accelerated in the presence of $Na[CL-14\cdot2H_2O]$.

Singh has reported the thermal decomposition of AN in the presence of transition metal salts of NTO [24]. The thermal decomposition of AN with these transition metal salts exhibits an exothermic peak in the DTA thermograms at 200 ^{o}C, which might be due to formation and dissociation of ammonium salts of NTO [24]. The similar phenomenon has not been found from the DSC curves of $AN/Na[CL-14\cdot2H_2O]$, which indicates a difference catalytic mechanism for AN catalyzed by $Na[CL-14\cdot2H_2O]$ and transition metal salts of NTO. Furthermore, $AN/Na[CL-14\cdot2H_2O]$ exhibits lower endothermic peak than that of AN with transition metal salts of NTO, which implies that $Na[CL-14\cdot2H_2O]$ exhibits higher catalytic activity on the thermal decomposition of AN [24].

Kinetic analyses (calculated by the Kissinger equation). It is widely considered that addition of catalyst lowers the activation energy (E_a) of the reaction [52]. E_a can provide reasonable information about the critical energy needed to start the decomposition reaction of the compound. A decrease in the E_a can be directly related to the catalytic activity of the catalyst under investigation. The isoconversional methods of kinetic analysis permit to explore the multistep kinetics of the thermal decomposition reactions and helps in drawing mechanistic conclusions about process material [53]. The DSC and kinetic parameters of the overall decomposition processes for pure AN and $AN/Na[CL-14\cdot2H_2O]$, calculated by Kissinger equation, were given in Table 5 [44]. In the present study, the E_a for pure AN yields a value of 91.6 kJ/mol,

which is in agreement with the reported value [15]. While a decrease in the E_a is observed for the completely decomposition process of AN/Na[CL-14·2H$_2$O]. It is widely considered that, the E_a of completely decomposition process for AN decomposition, associates with the intermediate products such as NH$_3$ and HNO$_3$ and a complete one to volatile products respectively [15]. Furthermore, in the present study, the thermal decomposition of AN and AN/Na[CL-14·2H$_2$O] is an endothermic process, as the heating rate rise then the absolute values of overall heat for the completely decomposition of AN and AN/Na[CL-14·2H$_2$O] decrease. In sharp contrast, the thermal decomposition of Na[CL-14·2H$_2$O] is an exothermic process, at the same heating rate, the absolute values of overall heat for the completely decomposition of AN/Na[CL-14·2H$_2$O] is lower than that of pure AN. It can be seen that Na[CL-14·2H$_2$O] increases the overall heat for the completely decomposition of AN. The above results indicate that Na[CL-14·2H$_2$O] dramatically influences the completely decomposition process of AN.

Kinetic analyses (calculated by the Ozawa equation). To predict the thermal decomposition mechanism of pure AN and AN/Na[CL-14·2H$_2$O], the corresponding extend of α-T (α is the extent of conversion, $0<\alpha<100$) kinetic curves (Fig. 4) were obtained by dealing the TG curves and compared. It can be seen that the thermal decomposition of AN/Na[CL-14·2H$_2$O] starts at lower temperature (about 30 $^{\circ}$C) than that of pure AN. This temperature difference points toward the AN decomposition catalyzed by Na[CL-14·2H$_2$O].

As is well know, the E_a calculated by the Kissinger equation is not enough to understand the whole thermal decomposition process of pure AN and AN/Na[CL-14·2H$_2$O]. Thus, we calculated E_a values of the decomposition reaction for pure AN and AN/Na[CL-14·2H$_2$O] by ozawa equation, and plotted of it against α [45-46]. As shown in Fig. 4, the E_a for pure AN yields a average value of 87.0 kJ/mol, which is approximately constant, suggests that the thermal decomposition mechanism for the whole process remains steady. Furthermore, the E_a value for pure AN calculated by ozawa equation is in good agreement with that of Kissinger equation. While, the mean E_a value required for the thermal decomposition of

AN/Na[CL-14·2H$_2$O] is 60.9 kJ/mol, which is significant lower than that of pure AN. This indicates some catalytic activity of Na[CL-14·2H$_2$O] on the preliminary decomposition of AN. The E_a for the decomposition (α between 5 and 20) is characterized by an average value of 74.6 kJ/mol, and the E_a keeps increasing, which indicates that the thermal decomposition mechanism of this region changes greatly. After α has reached 20, the E_a is approximately constant, the E_a for this region is characterized by an average value of 85.3 kJ/mol, suggests that the thermal decomposition mechanism of this region remains steady. The above results indicate that the thermal decomposition of AN catalyzed by Na[CL-14·2H$_2$O] requires lower E_a compared to that of non-catalyzed AN.

Possible mechanism of thermal decomposition of AN/Na[CL-14·2H$_2$O]. It is widely accepted that the decomposition of non-catalyzed AN follows two steps: NH$_3$ and HNO$_3$ are formed in the first step, then the HNO$_3$ further dissociates to smaller species [15]. Brower had demonstrated that, NH$_3$ and H$_2$O inhibit the AN decomposition and on the other hand HNO$_3$ promotes the decomposition [54]. The application of transition metal oxides can improve the low reactivity of AN and the catalytic activity can be enhanced by reducing their particle size [15].

$$NH_4NO_3 \rightarrow NH_3 + HNO_3 \qquad (6)$$

$$HNO_3 \rightarrow H_2O + NO_2 + NO + O_2 \qquad (7)$$
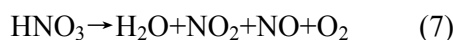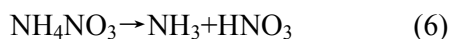
We have concluded that the main solid residues for thermal decomposition of Na[CL-14·2H$_2$O] are NaNCO and Na$_2$CO$_3$, respectively. And under certain conditions the NaNCO could split up or decompose into Na$_2$O, N$_2$ and CO [55]. More importantly, the thermal decomposition of AN catalyzed by Na[CL-14·2H$_2$O] in the region (α between 5 and 20) requires lower E_a compared to that of the other region(α between 20 and 95). This might indicate that Na[CL-14·2H$_2$O] most likely to catalyze the primary dissociation of AN into NH$_3$ and HNO$_3$, but not significant influence the secondary process involved in AN decomposition.

Work by Singh implies that the higher catalytic activity of the energetic additives for the thermal decomposition of propellants might be attributed to the fact that the active metal oxides are formed *in situ* in the system [29]. According to proton transfer

mechanism and work by Singh, we hypothesis that the Na[CL-14·2H$_2$O] decomposes and releases a amount of heat itself. This enhances the total heat of the AN mixture, as well as the formation of micro-sized and nano-sized Na$_2$CO$_3$ and Na$_2$O *in situ* on the AN surface. AN decomposition involves two steps: in the first step, Na$_2$O might promote the proton transfer process of AN, as the case that AP decomposition is catalyzed by p-type metal oxide [56]. In the second step, in presence of the micro-sized and nano-sized particles such as Na$_2$CO$_3$ and Na$_2$O, the evolved NH$_3$ might have undergone further absorption and reaction on the micro-sized and nano-sized Na$_2$CO$_3$ and Na$_2$O surfaces, consequently lowering the E_a of the process [10, 12-13, 57].

In general, Na[CL-14·2H$_2$O] used here could promote the completely decomposition of AN. Base on above results, we propose a possible mechanism of AN thermal decomposition catalyzed by Na[CL-14·2H$_2$O], as shown in Fig. 5.
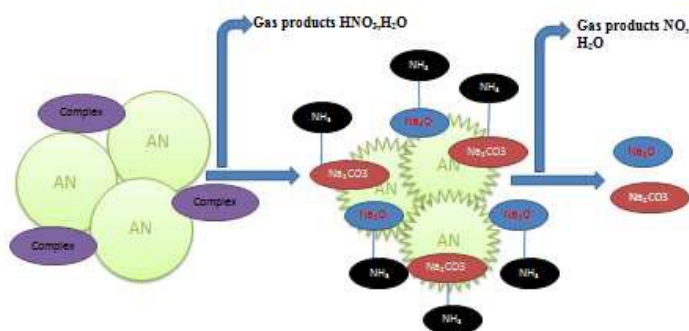

Fig. 5 A possible mechanism of AN thermal decomposition catalyzed by

Na[CL-14·2H$_2$O]

4. Conclusions

In conclusion, this study demonstrated a facile strategy to prepare a one-dimensional energetic complex constructed from sodium and CL-14, whose structure was characterized by X-ray diffraction. The crystal belongs to a monoclinic system with space group $P2_1$/c, and the complex possessed a one-dimensional coordination framework based on [ONaN]$_n$ chain, which might result in its good thermal and sensitive properties. Sensitivity test results show that the complex is classified as "less sensitive" energetic material. The thermal decomposition of the

complex contains one endothermic and one exothermic processes in the temperature range of 25-500 $^{\circ}$C with the NaNCO, Na_2CO_3, H_2O, NO and CO_2 as the final products. TG-DTG, TG-MS, DSC, α-T kinetic curves and thermal kinetic constants analyses show that the complex might be incorporated as a potential energetic catalyst in AN-based propellants.

References

1 T. Zhang, G. X. Li and Y. S. Yu, Energ Convers Manage., 2014, 87, 965.

2 C. Oommen and S. R. Jain, *J. Hazard. Mater*., 1999, **67**, 253.

3 S. Chaturvedi and P. N. Dave, *J. Energ. Mater*., 2013, **31**, 1.

4 M. Kohga and K. Okamoto, *Combust. Flame*., 2011, **158**, 573.

5 M. Pandey, S. Jha and R. Kumar, *J. Therm. Anal. Calorim*., 2012, **107**, 135.

6 V. P. Sinditskii and V. Y. Egorshev, *J. Propul. Power*., 2008, **24**, 1068.

7 N. Tomoki and K. Makoto, *Propell. Explos. Pyro*., 2013, **38**, 87.

8 N. Tomoki and K. Makoto, *Propul. Power*., 2014, **30**, 864.

9 K. Kajiyama, Y. Izato and A. T. Miyake, *J. Therm. Anal. Calorim*., 2013, **113**, 1475.

10 A. A. Vargeese, S. J. Mija and K. Muralidharan, *J. Energ. Mater*., 2014, **32**, 146.

11 M. Pandey, S. Jha and R. Kumar, *J. Therm. Anal. Calorim*., 2012, **107**, 135.

12 A. A. Vargeese, K. K. Muralidharan and V. N. Krishnamurthy, *Propell. Explos. Pyro*., 2014, **35**, 1

13 A. A. Vargeese and K. K. Muralidharan*, J. Hazard. Mater*., 2011, **192**, 1314.

14 E. Brian, R. A. Greiner and J. Frederick, *J. Propul. Power*., 2003,**19**, 713.

15 A. A. Vargeese and K. K. Muralidharan, *Appl. Catal. A: Gen*., 2012, **447**, 171.

16 S. Reshmi, K. B. Catherine and C. P. R. Nair, *Int. J. Nanotech*., 2011, **8**, 979.

17 P. Simoes, L. Pedroso and A. Portugal, *Propel. Explos. Pyro*., 2001, **26**, 278.

18 S. Ganesan and B. T. N. Sridhar, *Int. J. Mech & Mech. Eng*., 2014, **14**, 110.

19 H. Kazuo, *J. Energ. Mater*., 2014, **32**, 199.

20 K. Makoto and N. Saeko, *Propell. Explos. Pyro*., 2009, **34**, 340.

21 A. Miyake and Y. Izato, *J. Ener. Mater. Chem. Propul*., 2010, **9**, 523.

22 I. Yu-ichiro, M. Atsumi and D. Shingo, *Propell. Explos. Pyro*., 2013, **38**, 129.

23 K. Makoto, N. Tomoki and O. Kayoko, *Int. J. Aerosp. Eng*., 2012, 1.

24 G. Singh and S. P. Felix, *Combust. Flame*., 2003, **135**, 145.

25 G. Singh and S. P. Felix, *Combust. Flame*., 2003, **132**, 422.

26 J. H. Yi, F. Q. Zhao and W. L. Hong, *J. Hazard. Mater*., 2010, **176**, 257.

27 P. B. Kulkarni, T. S. Reddy and J. K. Nair, *J. Hazard. Mater*., 2005, **123**, 54.

28 P. B. Kulkarni, G. N. Purandare and J. K. Nair, *J. Hazard. Mater*., 2005, **119**, 53.

29 G. Singh and S. P. Felix, *J. Hazard. Mater*., 2002, **90**, 1.

30 X. Fan, J. Li and L. Zhang, *Chin. J. Energ. Mater*., 2007, **4**, 008.

31 J. Cheng, R. X. Zhang and Z. L. Liu, *RSC Adv*, 2015, **5**, 50278.

32 J. J. Liu, Z. L. Liu and J. Cheng, *J. Solid. State. Chem*., 2013,**197**, 198.

33 J. J. Liu, Z. L. Liu and J. Cheng, *RSC Adv.*, 2013, **3**, 2917.

34 J. J. Liu, Z. L. Liu and J. Cheng, *J. Solid. State. Chem.*, 2013, **200**, 43.

35 J. J. Liu, Z. L. Liu and J. Cheng, *Chin. J. Inorg. Chem*., 2014, **3**, 696.

36 W. P. NorrisU.S. Patent 5,039,812[P]. 1991-8-13.

37 A. K. Sikder, R. K. Sinha and B. R. Gandhe, *J. Hazard. Mater*., 2003, **102**, 137.

38 Mehilal, N. Sikder and S. K. Chougule, *J. Energ. Mater*., 2004, **22**, 117.

39 Impact: insensitive>40 J, less sensitive≥35, sensitive ≥ 4 J, very sensitive≤3 J; Friction insensitive>360 N, less sensitive=360 N, sensitive<360 N a. >80N, very sensitive ≤80 N, extremely sensitive≤10 N. According to: UN Recommendations of the Transport of Dangerous Goods. Manual of Tests and Criteria (Fourth revised ed.), NewYork and Geneva, United Nations, 2002, ST/SG/AC.10/11/Rev 4.

40 G. M. Sheldriclc, Crystal Structure Communications., 2001, **57**, 939.

41 G.M. Sheldriclc, SHELXS-97, Program for X-ray crystal structure refinement, university of gottingen, Germany,1997.

42 P. F. Pagoria, G. S. Lee and A. R. Mitchell, Thermochimica Acta, 2002, **384**, 187.

43 Y. Wang, S. Li and Y. Li, *J. Mater. Chem. A*., 2014, **2**, 20806.

44 H. E. Kissinger, *Anal. Chem.*, 1957, **29**, 1702.

45 T. Ozawa, *Chem. Bulletin. Chem. Soc. Jap.*, 1965, **38**, 1881.

46 C. D. Doyle, *J. Appl. Poly. Sci.*,1961, **5**, 285.

47 L. Yang, Chin J Chem.,2004, **22**, 1219.

48 J. Straszko, M. Olsok-Humienik and J. Mozejko, Thermochimica Acta., 1997, **292**, 145.

49 M. Olsok-Humienik and J. Mozejko, Thermochimica Acta., 2000, **344**, 73.

50 Z. R. Lu, Y. C. Ding and Y. Xu, Chin J Chem., 2004, **22**, 1091.

51 M. Fathollahi, S. M. Pourmortazavi and S. G. Hosseini, *J. Energ. Mater.*, 2008, **26**, 52.

52 A. K. Galwey, *Thermo. Acta.*, 2004, **413**, 139.

53 P. K. Reddy, A. C. K. Chowlu and A. K. Ghoshal, *Appl. Cata. A: Gen*, 2008, **351**, 195.

54 K. R. Brower, J. C. Oxley and M. Tewari, *J. Phys. Chem.*, 1989, **93**, 4029.

55 T. B. Brill, T. L. Zhang and B. C. Tappan, *Combust. Flame.*, 2000, **121**, 662.

56 S. A. Makhlouf, *J. Magn. Magn. Mater.*, 2002, **246**, 184.

57 M. Primet, P. Pichat and M. V. Mathieu, *J. Phys. Chem.*, 1971, **75**, 1221.